0026-895X/11/7901-51–60$20.00
MOLECULAR PHARMACOLOGY
Copyright © 2011 The American Society for Pharmacology and Experimental Therapeutics
Mol Pharmacol 79:51–60, 2011

Vol. 79, No. 1
68130/3651631
Printed in U.S.A.

Aminoglycosides Inhibit KCNQ4 Channels in Cochlear Outer Hair Cells via Depletion of Phosphatidylinositol(4,5)bisphosphate[S]

Michael G. Leitner, Christian R. Halaszovich, and Dominik Oliver

Department of Neurophysiology, Institute for Physiology and Pathophysiology, Philipps University of Marburg, Marburg, Germany

Received August 12, 2010; accepted October 8, 2010

ABSTRACT

Aminoglycoside antibiotics (AGs) are severely ototoxic. AGs cause degeneration of outer hair cells (OHCs), leading to profound and irreversible hearing loss. The underlying mechanisms are not fully understood. OHC survival critically depends on a specific K^+ conductance ($I_{K,n}$) mediated by KCNQ4 (Kv7.4) channels. Dysfunction or genetic ablation of KCNQ4 results in OHC degeneration and deafness in mouse and humans. As a common hallmark of all KCNQ isoforms, channel activity requires phosphatidylinositol(4,5)bisphosphate [PI(4,5)P_2]. Because AGs are known to reduce PI(4,5)P_2 availability by sequestration, inhibition of KCNQ4 may be involved in the action of AGs on OHCs. Using whole-cell patch-clamp recordings from rat OHCs, we found that intracellularly applied AGs inhibit $I_{K,n}$. The inhibition results from PI(4,5)P_2 depletion indicated by fluorescence imaging of cellular PI(4,5)P_2 and the dependence of inhibition on PI(4,5)P_2 availability and on PI(4,5)P_2 affinity of recombinant KCNQ channels. Likewise, extracellularly applied AGs inhibited $I_{K,n}$ and caused substantial depolarization of OHCs, after rapid accumulation in OHCs via a hair cell-specific apical entry pathway. The potency for PI(4,5)P_2 sequestration, strength of $I_{K,n}$ inhibition, and resulting depolarization correlated with the known ototoxic potential of the different AGs. Thus, the inhibition of $I_{K,n}$ via PI(4,5)P_2 depletion and the resulting depolarization may contribute to AG-induced OHC degeneration. The KCNQ channel openers retigabine and zinc pyrithione rescued KCNQ4/$I_{K,n}$ activity from AG-induced inhibition. Pharmacological enhancement of KCNQ4 may thus offer a protective strategy against AG-induced ototoxicity and possibly other ototoxic insults.

Introduction

Aminoglycoside antibiotics (AGs) are highly efficient in the treatment of infections caused by Gram-negative bacteria, but clinical use is restricted by severe ototoxic side effects (Forge and Schacht, 2000; Rybak and Ramkumar, 2007). The hearing loss induced by clinical doses of AGs results from degeneration of OHCs and is therefore profound and irreversible. Inner hair cells (IHCs) show little vulnerability to AGs, and susceptibility of OHCs shows a marked cochlear base-to-apex gradient. Basal, high-frequency OHCs are most sensitive, which leads to initial high-frequency hearing loss that proceeds to lower frequencies with continued administration of AGs (Fausti et al., 1984). AG-induced ablation of OHCs is also widely used to study hair cell regeneration in animal models. However, the underlying mechanisms are not fully understood, and the basis of the differential susceptibility of hair cells remains elusive.

Hair cell damage occurs after the uptake of AGs from the endolymph via endocytosis or mechanoelectrical transduction (MET) channels (Hashino and Shero, 1995; Marcotti et al., 2005). After entry, AGs seem to initiate multiple pathways, leading to necrotic or apoptotic cell death. These pathways may involve caspase-dependent and -independent signals (Jiang et al., 2006a), formation of reactive oxygen species (Rybak and Ramkumar, 2007), mitochondrial dysfunction (Dehne et al., 2002), and disruption of phosphoinositide homeostasis (Jiang et al., 2006b; Goodyear et al., 2008). In addition, it is known that AGs interact with phosphoinositides via strong electrostatic interactions and can thereby functionally deplete these phospholipids (Gabev et al., 1989).

OHC function is directly linked to phosphoinositide metabolism, because the major K^+ current of OHCs, $I_{K,n}$, is mediated by KCNQ4 (Kv7.4) channels (Kubisch et al., 1999; Kharkovets et al., 2000, 2006). Activity of all KCNQ isoforms,

This work was supported by the Deutsche Forschungsgemeinschaft [Grants SFB 593, TP A12]; and by the University Medical Center Giessen and Marburg [Grant 42/2010 MR].

Article, publication date, and citation information can be found at http://molpharm.aspetjournals.org.

doi:10.1124/mol.110.068130.

[S] The online version of this article (available at http://molpharm.aspetjournals.org) contains supplemental material.

ABBREVIATIONS: AG, aminoglycoside antibiotic; OHC, outer hair cell; IHC, inner hair cell; PI(4,5)P_2, phosphatidylinositol(4,5)bisphosphate; TR, Texas Red fluorescent dye; NTR, neomycin Texas Red conjugate; GTTR, gentamicin Texas Red conjugate; MET, mechanoelectrical transduction; GFP, green fluorescent protein; TIRF, total internal reflection; CHO, Chinese hamster ovary; ZnP, zinc pyrithione; XE991, 10,10-*bis*(4-pyridinylmethyl)-9(10*H*)-anthracenone dihydrochloride.

including KCNQ4, essentially depends on $PI(4,5)P_2$ (Li et al., 2005; Suh et al., 2006). Strikingly, $I_{K,n}$/KCNQ4 activity is essential for OHC survival. Pharmacological block and genetic ablation of KCNQ4 result in OHC degeneration and hearing loss (Nouvian et al., 2003; Kharkovets et al., 2006). Remarkably, this degeneration totally resembles AG-induced outer hair cell loss, starting at the cochlear basis and proceeding to the apex. Mutations of KCNQ4 underlie the human hereditary deafness, DFNA2, further highlighting the importance of KCNQ4 for hair cell maintenance (Kubisch et al., 1999; Kharkovets et al., 2000).

Bringing together the knowledge on KCNQ channel regulation, interaction of AGs with phosphoinositides, and dependence of OHC survival on KCNQ4 leads to the idea that $I_{K,n}$ may be a primary molecular target of ototoxic AGs. Given the important implications for the etiology of AG-induced hair cell loss, we analyzed the effect of AGs on OHC currents and recombinant KCNQ4. We find that both are inhibited by intracellular AGs. Imaging of $PI(4,5)P_2$ concentrations, experimental manipulation of $PI(4,5)P_2$ levels, and differential responses of KCNQ isoforms with different $PI(4,5)P_2$ affinities indicate that this inhibition results from depletion of free $PI(4,5)P_2$. Moreover, entry of AGs into OHCs through stereociliary MET channels is sufficient to substantially block $I_{K,n}$ and to depolarize the hair cell. Thus, inhibition of $I_{K,n}$ may contribute to AG ototoxicity.

Materials and Methods

Acute Organ of Corti Preparation. Animals were kept according to German law and institutional guidelines at the Philipps University (Marburg, Germany). Apical cochlear turns of Wistar rats (12–20 days after birth) were isolated as described previously (Oliver et al., 2000). The preparation was placed in a recording chamber and continuously perfused with standard extracellular solution containing 144 mM NaCl, 5.8 mM KCl, 1.3 mM $CaCl_2$, 0.9 mM $MgCl_2$, 0.7 mM NaH_2PO_4, 10 mM HEPES, and 5.6 mM D-glucose, pH 7.4 (adjusted with NaOH), 305 to 310 mOsmol/kg. Experiments were performed within 3 h after the preparation.

Cell Culture and Transfection. Chinese hamster ovary (CHO) cells were platted on glass coverslips and transfected with jetPEI (Polyplus Transfection, Illkirch, France). The following expression vectors were used: pEGFP-C1-KCNQ4 (NM_004700.2); pBK-CMV-KCNQ3 (NM_004519.2) (plus pEGFP for identification of transfected cells); and pEGFP-C1-tubby-Cterm (NP_068685.1, amino acids 243–505) pRFP-C1-PI(4)P-5 kinase (NM_008846.1). Experiments were performed 24 to 48 h after transfection.

Electrophysiological Recordings from OHCs and CHO Cells. Whole-cell recordings were done with an Axopatch 200B amplifier (Molecular Devices, Sunnyvale, CA) in voltage-clamp or current-clamp mode. Data were sampled with an ITC-18 interface (HEKA, Lambrecht/Pfalz, Germany) controlled by PatchMaster software (HEKA). Currents were low pass-filtered at 2 kHz and sampled at 5 kHz. Patch pipettes were pulled from quartz glass to an open pipette resistance of 1.5 to 3 MΩ when filled with intracellular solution containing 135 mM KCl, 2.41 mM $CaCl_2$ (free Ca^{2+}, 0.1 μM), 3.5 mM $MgCl_2$, 5 mM HEPES, 5 mM EGTA, and 2.5 mM Na_2ATP, pH 7.3 (adjusted with KOH), 290 to 295 mOsmol/kg. In some experiments, neomycin trisulfate, kanamycin disulfate, G418 (Geneticin) disulfate, or poly(D-lysine) hydrobromide (molecular weight, 1000–4000) (all from Sigma-Aldrich, Munich, Germany) was added to the intracellular solution at the concentrations indicated under *Results*. Series resistance (R_S) was less than 10 MΩ, and R_S compensation (80–90%) was applied. For perforated patch-clamp experiments, pipettes were pulled from borosilicate glass to an open pipette resistance of 1.5 to 3 MΩ. Pipettes were tip-filled with standard intracellular solution and then back-filled with the same solution containing 120 μg/ml Nystatin (Sigma-Aldrich). R_S was less than 22 MΩ, and R_S compensation (75%–80%) was applied.

Experiments were performed on OHCs of the third row. Access to the basolateral membrane was achieved by gently removing adjacent supporting cells with a suction pipette. Only OHCs with visually intact stereocilia and a membrane potential more negative than −69 mV were used. Neomycin trisulfate, kanamycin disulfate, 10,10-*bis*(4-pyridinylmethyl)-9(10*H*)-anthracenone dihydrochloride (XE991), zinc-pyrithione (all purchased from Sigma-Aldrich), and retigabine (kindly provided by Neurosearch, Ballerup, Denmark) were added to the extracellular solution at the concentrations indicated under *Results* and applied locally via a glass capillary. All experiments were performed at room temperature. Membrane potentials shown are not corrected for liquid junction potential (−4 mV).

Total Internal Reflection Imaging. Total internal reflection (TIRF) microscopy was performed as described previously (Halaszovich et al., 2009). In brief, experiments were performed using a BX51WI upright microscope (Olympus, Hamburg, Germany) equipped with a TIRF condensor (numerical aperture of 1.45; Olympus) and a 488 nm laser (20 mW; Picarro, Sunnyvale, CA). Fluorescence was imaged by a LUMPlanFI/IR 40X/0.8 water immersion objective (Olympus). Fluorescence was acquired with an IMAGO-QE cooled charge-coupled device camera controlled by TILLvisION software (TILL Photonics, Gräfelfing, Germany). CHO cells transiently expressing Tubby-Cterm-GFP (Santagata et al., 2001; Halaszovich et al., 2009) were simultaneously imaged and voltage-clamped. Experiments were included for analysis when the access resistance was less than 5 MΩ to ensure consistent and rapid dialysis of AGs. F/F_0 traces were calculated from the background-corrected TIRF signal (F) and initial fluorescence intensity (F_0), averaged over the footprint of the patch-clamped cell excluding cell margins to avoid movement artifacts.

Aminoglycoside Labeling and Confocal Microscopy. Gentamicin and neomycin (both from Sigma-Aldrich) were conjugated with Texas Red (TR) according to published protocols (Sandoval et al., 1998). In brief, gentamicin sulfate or neomycin trisulfate (both 50 mg/ml in 100 mM K_2CO_3, pH 8.5) were agitated with Texas Red-X succinimidyl ester (TR; Invitrogen, Carlsbad, CA) at a molar ratio of 330:1 for 36 h at 4°C (final AG concentration, 50 mM; final TR, concentration 0.150 mM). As a control, TR was diluted in 100 mM K_2CO_3, pH 8.5, and processed accordingly. The obtained gentamicin-Texas Red (GTTR) and neomycin-Texas Red (NTR) conjugates were diluted (1:50) to final concentrations of 1 mM with standard extracellular solution. Control TR solution was diluted accordingly to obtain equal concentrations of the fluorescent dye in control experiments (1:50). For some experiments, NTR was diluted in extracellular solution containing 144 mM KCl, 5.8 mM NaCl, 1.3 mM $CaCl_2$, 0.9 mM $MgCl_2$, 0.7 mM NaH_2PO_4, 10 mM HEPES, and 5.6 mM D-glucose, pH 7.4 (adjusted with NaOH), 305 to 310 mOsmol/kg.

Confocal live-cell imaging was performed with an upright LSM 710 Axio Examiner.Z1 microscope equipped with a W Plan/Apochromat 20×/1.0 DIC M27 75-mm water immersion objective (Carl Zeiss GmbH, Jena, Germany). Texas Red was excited at 561 nm with a diode-pumped solid-state laser (Carl Zeiss), and fluorescence emission was sampled at 565 to 609 nm. All preparations were imaged with the same laser power and gain settings. Fluorescence was averaged from regions of interest at various levels of OHCs, background-corrected, and is presented normalized to the initial background fluorescence F_0 at the beginning of an experiment.

Data Analysis and Statistics. Electrophysiological data were analyzed using PatchMaster (HEKA) and IGOR Pro (Wavemetrics, Lake Oswego, OR). Recombinant KCNQ current amplitudes were derived from monoexponential fits to current activation at 0 mV. $I_{K,n}$ was activated at a holding potential of −60 mV, and the current was

quantified as the XE991-sensitive tail current amplitude from this holding potential at −130 mV and corrected for leak current remaining after channel deactivation. Different voltage protocols were used for recombinant KCNQ4 and $I_{K,n}$ to account for the large difference in their activation voltage ranges (Kubisch et al., 1999; Marcotti and Kros, 1999).

Fluorescence time series were analyzed using TILLvisION (TILL Photonics), Zen 2009 (Carl Zeiss), ImageJ (http://rsbweb.nih.gov/ij/), and Igor Pro (Wavemetrics).

Statistical analysis was performed with (paired) *t* test, and significance was assigned at $P \leq 0.05$. Data are presented as mean ± S.E.M., with *n* representing the number of independent experiments (individual cells).

Results

Inhibition of $I_{K,n}$ and KCNQ4 by Intracellular Aminoglycosides. Because hair cell degeneration occurs after the entrance and cytoplasmic accumulation of AGs (Hiel et al., 1993; Hashino and Shero, 1995), we first analyzed the effects of intracellular AGs on $I_{K,n}$ by introducing AGs through the patch pipette. $I_{K,n}$ current amplitude was measured as the deactivating tail current at −130 mV sensitive to the KCNQ channel blocker XE991 (Fig. 1A), showing that the used voltage protocol is qualified to monitor the KCNQ conductance in OHCs.

After the establishment of the whole-cell configuration, KCNQ4-mediated currents rapidly decreased by approximately 60% of initial amplitude, when the prototypical AG, neomycin (1 mM) was included in the pipette solution (Fig. 1, B and C). In contrast, only minor channel rundown was observed in the absence of neomycin (Fig. 1D). These results indicate the inhibition of $I_{K,n}$ by neomycin entering the cell. As shown in Fig. 1F, patching OHCs with various neomycin concentrations yielded dose-dependent inhibition of $I_{K,n}$ with a half-blocking concentration of 0.59 mM. XE991-insensitive K^+ currents in OHCs that are not carried by KCNQ channels were not affected by neomycin (Supplemental Fig. S1).

Other AG antibiotics were also tested for their effect on $I_{K,n}$. Both G418 (an AG that is similar in structure to gentamicin) and kanamycin inhibited $I_{K,n}$, albeit with lower potency than neomycin (35 and 30% at 1 mM, respectively; Fig. 1, E and G). Poly(D-lysine) (200 μg/ml), another polycationic molecule, which is structurally unrelated to AGs, strongly inhibited $I_{K,n}$ when applied via the pipette (Fig. 1G). In contrast, ampicillin, a structurally unrelated antibiotic that lacks net positive charge, had no effect on $I_{K,n}$. These findings suggest that the polycationic nature of AGs is essential for the inhibiting effect on $I_{K,n}$. The rapid time course of inhibition suggested an immediate action of AGs on the channels rather than involvement of intracellular signaling pathways that have been implicated in AG action.

We therefore examined the interaction of AGs with KCNQ4 in a simple recombinant system. Whole-cell voltage-clamp experiments were done on CHO cells heterologously expressing KCNQ4. The introduction of neomycin via the patch pipette robustly inhibited KCNQ4 currents (Fig. 2, B and E). Sensitivity toward neomycin was somewhat higher than observed in hair cells, yielding a half-inhibiting concentration of 0.13 mM (Fig. 2D). Similar to native $I_{K,n}$, G418,

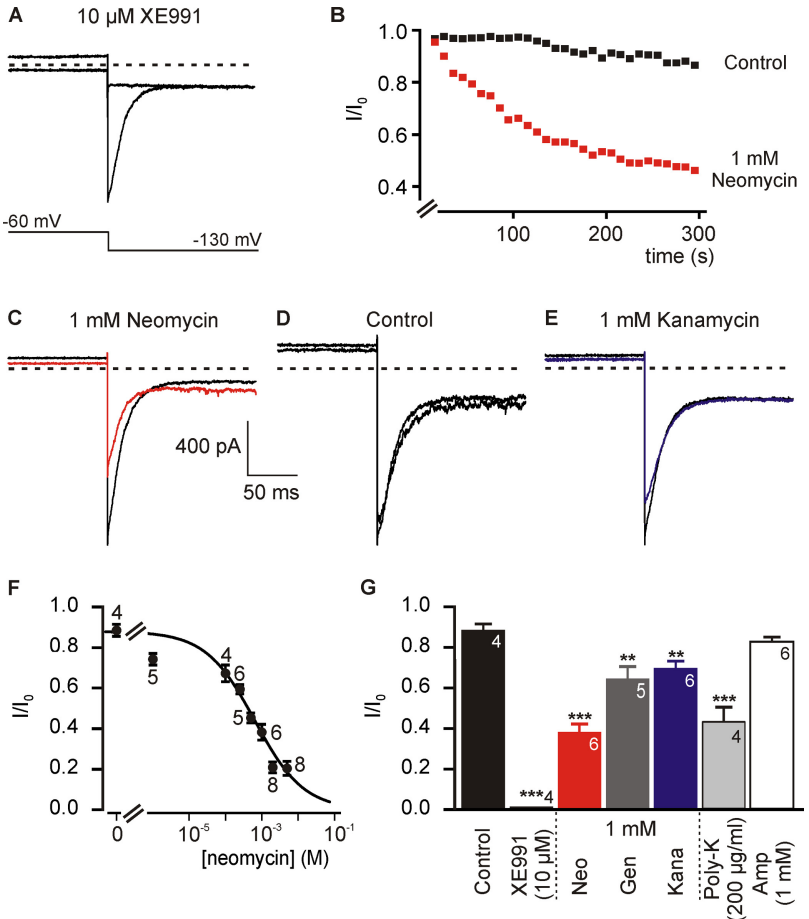

Fig. 1. Intracellular aminoglycoside antibiotics inhibit $I_{K,n}$. A, $I_{K,n}$, measured from rat OHCs as the deactivating inward tail current upon hyperpolarization (voltage command as indicated). Complete block by application of XE991 identifies this current as being carried by KCNQ channels. B, time course of current amplitude after establishment of whole-cell configuration in the absence (black) and presence (red) of neomycin in the pipette solution. Traces are representative recordings obtained from two different OHCs. Currents are presented normalized to the amplitude immediately after patch rupture (I_0). C, D, and E, representative currents immediately (black) and 10 min after (colored) patch rupture obtained with pipette solutions containing neomycin (C), no aminoglycosides (control; D) or kanamycin (E). Scale bars apply to A, C, D, and E. F, dose-dependent inhibition of $I_{K,n}$ by intracellular neomycin measured as in C. Continuous line shows a fit with the Hill equation, yielding an IC_{50} of 0.59 mM and a Hill coefficient of 1.3. G, steady-state inhibition of $I_{K,n}$ by various antibiotics and polycations. Neo, neomycin; Gen, G418; Kana, kanamycin; poly-K, poly(D-lysine); Amp, ampicillin. Numbers of experiments are indicated. **; $P \leq 0.01$; ***, $P \leq 0.001$.

kanamycin, and poly(D-lysine) also inhibited recombinant KCNQ4, whereas ampicillin was ineffective (Fig. 2E). The order of sensitivities toward these polycations was the same obtained from hair cells, suggesting the same mechanism of inhibition for $I_{K,n}$ and recombinant KCNQ4.

Aminoglycosides Interfere with the Availability of PI(4,5)P_2 to Channels. It is well established that neomycin and poly(D-lysine) bind PI(4,5)P_2 via electrostatic interaction with the anionic head groups (Gabev et al., 1989), thereby effectively chelating these lipids. Because activity of all KCNQ channels requires binding of PI(4,5)P_2, inhibition of $I_{K,n}$ may result from reduced availability of PI(4,5)P_2 to the channels. Indeed, sequestration by polycations has been used previously to define the role of phosphoinositides in the regulation of ion channels (Oliver et al., 2004; Suh and Hille, 2007).

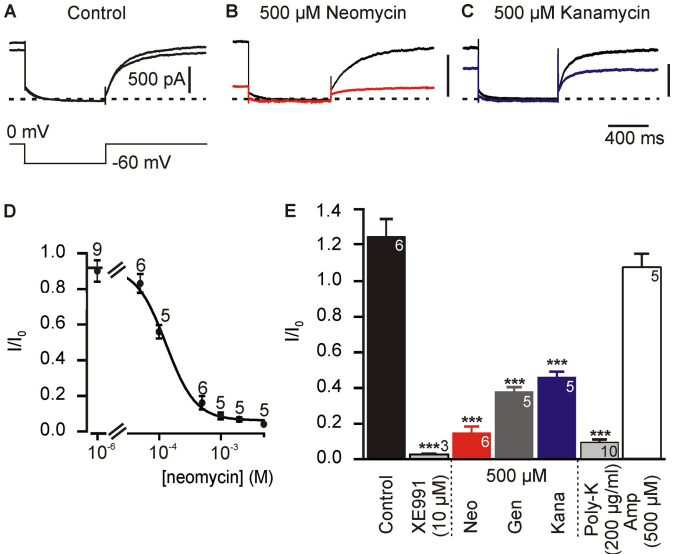

Fig. 2. Inhibition of recombinant KCNQ4 channels by intracellular aminoglycosides. A, representative whole-cell currents recorded from a CHO cell transiently expressing homomeric KCNQ4 channels, immediately (top trace) and 10 min after establishment of whole-cell configuration. Voltage protocol was performed as indicated in inset. B and C, recordings as in A with neomycin (B) or kanamycin (C) included in the patch pipette solution. Steady-state currents after dialysis of aminoglycosides into the cell are indicated in color. D, dose-dependent inhibition of KCNQ4 by intracellular neomycin measured as in B. Steady-state currents were normalized to current amplitude immediately after patch rupture (I_0) for each cell. Fit of the Hill equation to the data set (continuous line) yields IC_{50} of 0.13 mM and Hill coefficient of 1.8. E, summarized steady-state inhibition of KCNQ4 by the various antibiotics and polycations indicated. ***, $P \leq 0.001$.

To address the involvement of PI(4,5)P_2 in AG-induced inhibition of $I_{K,n}$/KCNQ4, we first examined the ability of AGs to effectively deplete free PI(4,5)P_2 under our experimental conditions. To this end, we used a genetically encoded sensor for PI(4,5)P_2, the GFP-fused C terminus of the tubby protein (tubby-Cterm) (Santagata et al., 2001; Halaszovich et al., 2009). The degree of binding of this protein domain to the plasma membrane is a direct measure for the concentration of free PI(4,5)P_2. We measured membrane association of Tubby-Cterm using total internal reflection (TIRF) microscopy as described previously (Halaszovich et al., 2009). In brief, TIRF was used to selectively excite GFP bound to the plasma membrane, such that the obtained fluorescence signal directly reported the amount of membrane-associated PI(4,5)P_2 sensor and thus the concentration of free PI(4,5)P_2. As before, cells were dialyzed with either neomycin or kanamycin via a patch pipette (1 mM each). Upon the introduction of neomycin into the cell, the TIRF signal rapidly decreased to 26% of the initial signal amplitude, reporting full dislocation of Tubby from the membrane (Halaszovich et al., 2009) and thus depletion of free PI(4,5)P_2 (Fig. 3, A and B). In contrast, without neomycin in the pipette (control, Fig. 3, A and B) only an initial minor reduction of membrane fluorescence was observed, probably because of washout and bleaching of the fluorescent probe upon rupture of the membrane patch. Kanamycin also reduced free PI(4,5)P_2 concentration (to 70%), as indicated by a decrease of membrane fluorescence exceeding control recordings (Fig. 3, A and B).

However, the change of the TIRF signal and thus reduction of PI(4,5)P_2 concentration was significantly smaller than that observed with the same concentration of neomycin (Fig.

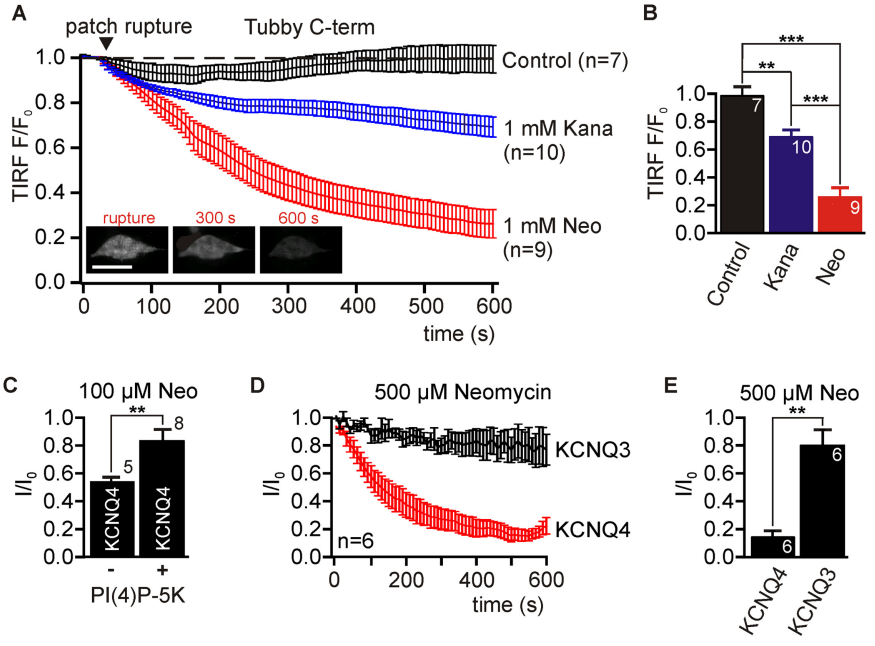

Fig. 3. Aminoglycosides decrease free PI(4,5)P_2 in the plasma membrane. A, combined TIRF imaging and patch-clamp experiments on CHO cells transfected with the PI(4,5)P_2 sensor domain Tubby-Cterm. Fluorescence intensity (TIRF F/F_0) signifies the degree of membrane association of the sensor, and is shown normalized to signal intensity (F_0) before establishing whole-cell configuration (patch rupture). Note that inclusion of neomycin and kanamycin in the patch pipette displaced the PI(4,5)P_2 sensor from the membrane. Representative TIRF images of Tubby-Cterm are shown at three time points with neomycin applied via the patch pipette (inset; scale bar, 20 μm). B, averaged relative changes in TIRF signals upon introduction of aminoglycosides into CHO cells. C, coexpression of a constitutively active PI(4)P-5 kinase significantly attenuated neomycin-induced KCNQ4 current inhibition in CHO cells. Voltage-clamp experiments were performed as in Fig. 2. D and E, differential inhibition of homomeric KCNQ4 and KCNQ3 channels by aminoglycosides. D, whole-cell currents during introduction of 500 μM neomycin through the patch pipette were measured and normalized as in Fig. 2. E, steady-state inhibition of KCNQ4, characterized by low PI(4,5)P_2 affinity, is significantly stronger than inhibition of KCNQ3, exhibiting high PI(4,5)P_2 affinity. **; $P \leq 0.01$; ***, $P \leq 0.001$.

3B). Thus, the efficacy of both AGs for shielding $PI(4,5)P_2$ corresponds to the potency of KCNQ4 channel inhibition, consistent with the idea that inhibition results from depletion of $PI(4,5)P_2$.

If so, the degree of channel inhibition by AGs should depend on the $PI(4,5)P_2$ concentration in the plasma membrane. We therefore increased $PI(4,5)P_2$ levels in CHO cells by coexpression of a PI(4)P-5 kinase (e.g., Li et al., 2005; Suh and Hille, 2007). In these cells, the degree of KCNQ4 current inhibition by neomycin (100 μM) was significantly reduced compared with control cells (Fig. 3C).

The different KCNQ channel subtypes show marked differences in their apparent $PI(4,5)P_2$ binding affinities. Thus, homomeric KCNQ3 channels display a more than 50-fold higher apparent affinity compared with KCNQ4, rendering KCNQ4 more sensitive to $PI(4,5)P_2$ depletion than KCNQ3 (Li et al., 2005; Hernandez et al., 2009). We therefore compared the sensitivity of both channels to neomycin inhibition. As shown in Fig. 3, D and E, neomycin inhibition matched the channels' $PI(4,5)P_2$ affinity: KCNQ4 currents decreased to 14.9 ± 4.0% (n = 6) upon diffusion of 500 μM neomycin into the cells, whereas KCNQ3 currents were only slightly affected (reduction to 80.6 ± 10.6%, n = 6). Taken together, these findings strongly indicate that AGs inhibit KCNQ4 channels via the sequestration of $PI(4,5)P_2$ in the plasma membrane.

Extracellular Aminoglycosides Inhibit $I_{K,n}$ in OHCs but Not KCNQ4 in CHO Cells. In the above experiments, we directly delivered AGs into the OHC's cytoplasm. However, in an ototoxic insult, AGs reach the hair cells from the endolymph (Hashino and Shero, 1995; Wang and Steyger, 2009). We thus tested whether entry of AGs from the extracellular space is sufficient to induce substantial inhibition of $I_{K,n}$.

Extracellular application of neomycin (1 mM) onto OHCs robustly inhibited $I_{K,n}$ to 65.8 ± 1.6% (n = 12) of preapplication current amplitude. Representative current traces, time course of current inhibition, and mean inhibition are shown in Fig. 4, A, B, and C, respectively.

In contrast, application of kanamycin (1 mM) only slightly diminished $I_{K,n}$ current amplitudes (to 87.0 ± 2.0%, n = 9). However, this reduction was not significantly different from the slight current rundown observed in control experiments (to 93.4 ± 1.1%, n = 8) (Fig. 4, B and C). The current inhibition induced by the application of neomycin was not fully reversible, consistent with the uptake into the OHC and intracellular retention after extracellular wash-off (Fig. 4A). Because intracellular accumulation of AGs may be limited under whole-cell conditions by diffusional loss into the patch pipette, we performed additional recordings in the perforated patch configuration, preventing any washout of neomycin. Under perforated-patch conditions, application of neomycin

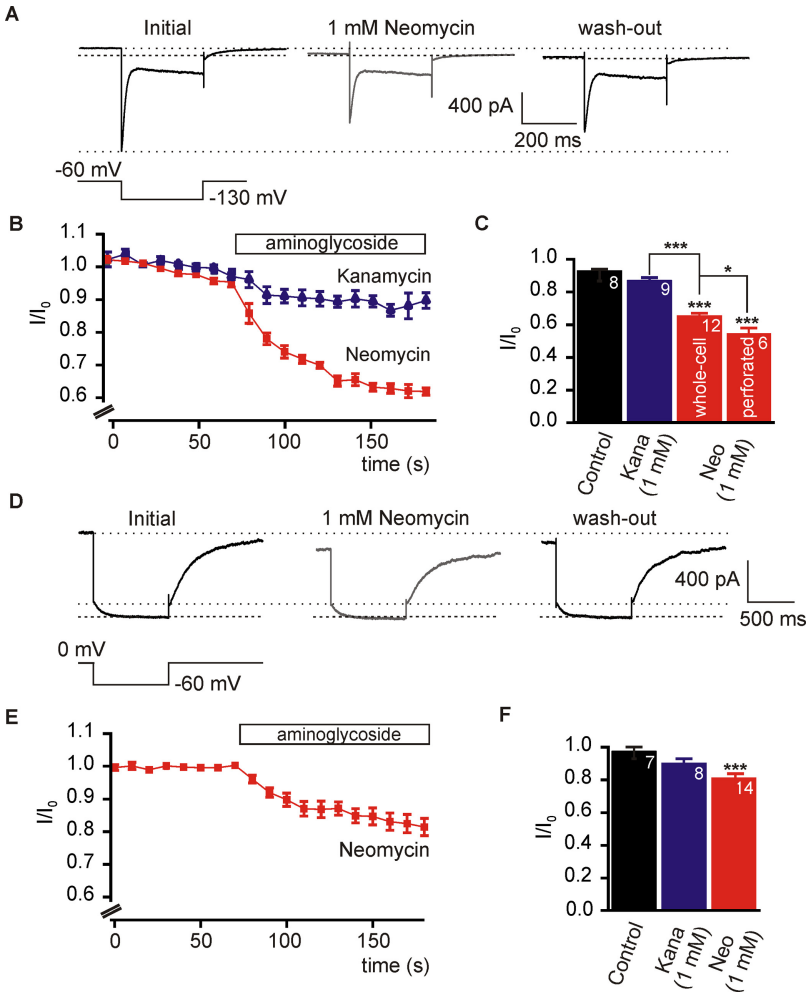

Fig. 4. Inhibition of $I_{K,n}$ in OHCs by extracellular aminoglycosides. A, representative current traces of $I_{K,n}$ before (left), during (middle), and after the extracellular application of neomycin (right). B, averaged time course of current amplitudes upon application of neomycin (1 mM, red) and kanamycin (1 mM, blue) onto OHCs, obtained as shown in A. C, summary of steady-state inhibition by extracellular aminoglycosides measured either in whole-cell or perforated-patch configuration. Note that inhibition by neomycin was significantly increased in the perforated-patch configuration compared with whole-cell. D, E, and F, effect of extracellular aminoglycosides on recombinant KCNQ4 channels expressed in CHO cells. D, representative whole-cell current traces before, during, and after application of neomycin. E, time course of currents upon application of neomycin. F, summary of relative steady state current amplitudes. Measurements were done in whole-cell configuration. *, $P \leq 0.05$; ***, $P \leq 0.001$.

induced a stronger inhibition of $I_{K,n}$ to 54.9 ± 3.7% (n = 6) compared with whole-cell recordings (P = 0.02), as shown in Fig. 4C. This finding is consistent with a higher degree of intracellular accumulation of the AG and thus supports an intracellular action of AGs on $I_{K,n}$.

To further scrutinize this conclusion, we also examined the effect of neomycin applied onto recombinant KCNQ4 channels in CHO cells, which lack the specific AG entry pathways of hair cells (Supplemental Fig. S2). Application of neomycin (1 mM) only slightly reduced KCNQ4 currents in a partially reversible manner (Fig. 4, D–F). Combined with the earlier finding of a substantially higher sensitivity of recombinant KCNQ4 to intracellular application of AGs, this result confirmed that AGs inhibit KCNQ4 only after uptake into the cell and do not considerably block channels from the extracellular side.

In summary, these results suggest that AGs inhibit KCNQ4-mediated $I_{K,n}$ after uptake and possibly accumulation via a hair cell-specific specific entry pathway.

Aminoglycoside Uptake into OHCs Is Fast. Although inhibition of $I_{K,n}$ by intracellular AGs is entirely consistent with the previously described entry of AGs into OHCs, the fast time course of current inhibition seemed surprising. Imaging studies are consistent with fast entry of AGs (Tiede et al., 2009); however, to our knowledge, the kinetics of AG entry have not been examined in detail at the relevant time scale.

Uptake of AGs into hair cells has been monitored previously using fluorescent Texas Red-derivatives of gentamicin (GTTR) (Dai et al., 2006). We used this approach to quantitatively record the entry of neomycin into OHCs in acutely isolated organs of Corti by confocal microscopy. Incubation with NTR or GTTR (1 mM each) for 5 min produced robust fluorescence inside OHCs and IHC but not in supporting cells and surrounding tissue (Fig. 5, A and B). Incubation with Texas Red alone did not increase hair cell fluorescence (Fig. 5C), confirming that the observed accumulation results from hair cell-specific entry of AGs but not from an unspecific permeation of the fluorescent group.

As shown in Fig. 5D, time-resolved imaging revealed the rapid accumulation of intracellular NTR in OHCs. Fluorescence increase was fastest and most pronounced in confocal sections through the hair bundles (time constant obtained from monoexponential fit to fluorescence increase, 69 s) and somewhat slower in optical sections through the medial and basal (subnuclear) regions of hair cells (281 and 241 s, respectively). These findings point to AG entry into OHCs at the level of the stereocilia and subsequent intracellular diffusion to the OHC's base, where $I_{K,n}$/KCNQ4 is located (Kharkovets et al., 2000).

AGs may enter via the hair cell's MET channels located at the stereociliary tips (Marcotti et al., 2005). Consequently, apical membrane potential must contribute to the driving force for permeation, with hyperpolarization increasing the rate of entry of these cationic molecules. We addressed voltage-dependence of AG uptake by applying NTR while depolarizing or hyperpolarizing the cells with high or low extracellular K^+ concentrations, respectively (Fig. 5, E and F). When NTR was applied to OHCs depolarized by 144 mM extracellular K^+, cellular fluorescence increased slowly (relative increase in the subnuclear region of OHCs, 0.02 s^{-1}). Subsequent hyperpolarization upon washout of extracellular

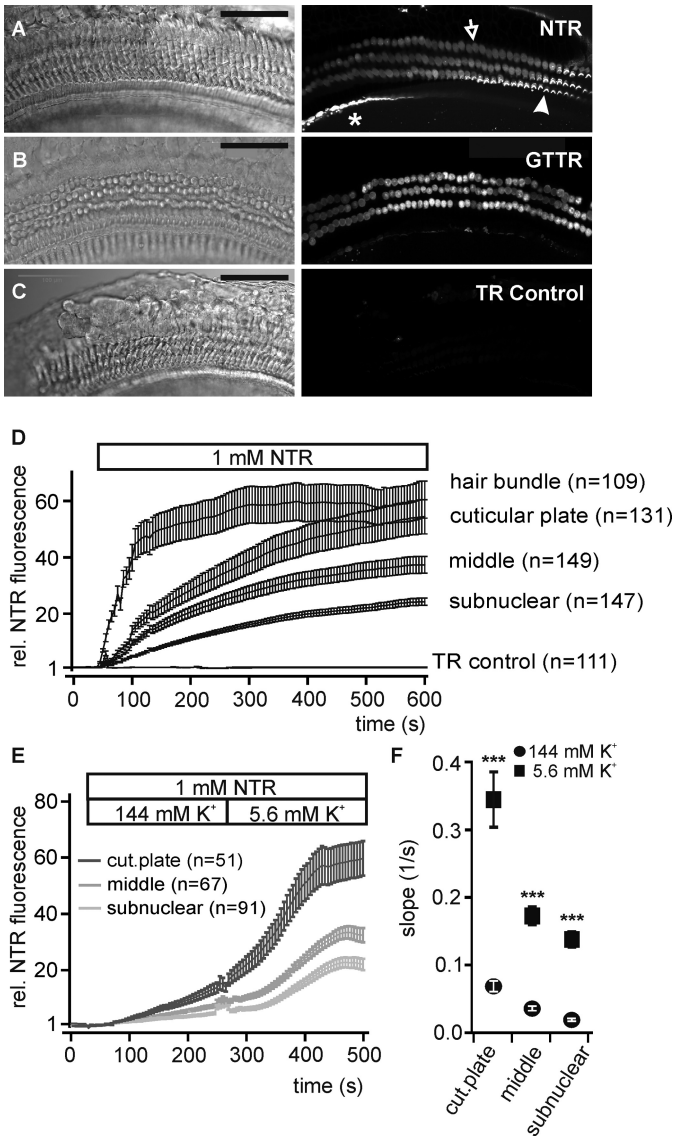

Fig. 5. Confocal imaging reveals rapid and voltage-dependent entry of aminoglycosides into OHCs. A, representative differential interference contrast (left) and confocal fluorescence (right) images of an isolated organ of Corti from rat, after incubation with fluorescently labeled neomycin (NTR; 1 mM) for 5 min (at room temperature). Note the selective uptake of NTR into OHCs and inner hair cells (∗). The oblique orientation of the preparation allows visualization of labeled OHC hair bundles (filled arrow) and cell bodies (open arrow) (scale bars, 100 μm). B, images as in A after application of fluorescently labeled gentamicin (GTTR; 1 mM). C, no increase of cellular fluorescence was detected upon application of Texas Red not conjugated to aminoglycosides (TR; same TR concentration as in A and B). D, time course of entry of NTR (1 mM) into OHCs. Fluorescence intensities were sampled from confocal optical sections through hair bundles, apical region (level of the cuticular plate), middle, and subnuclear regions of OHCs. Application of TR did not produce any detectable increase in fluorescence (bottom trace). Numbers of individual OHCs analyzed are indicated (from five independent preparations). E, voltage dependence of NTR entry. Increase of OHC fluorescence during application of NTR (1 mM) was slow in depolarizing extracellular medium (144 mM KCl) and accelerated upon exchange by repolarizing medium (5.6 mM KCl). Note that the onset of increased entry is delayed because of the time needed for full solution exchange in the recording chamber. F, quantification of NTR uptake kinetics. Relative increase was derived from linear fits to the fluorescence traces from single OHCs (n = 51–91, from four independent preparations). Asterisks indicate significantly faster fluorescence increase at 5.6 mM K^+ compared with 144 mM K^+. ∗∗∗, $P \leq 0.001$.

K^+ resulted in acceleration of fluorescence buildup (relative increase, 0.14 s^{-1}), indicating a strongly increased rate of aminoglycoside entry. Note that the onset of accelerated entry upon hyperpolarization is delayed because of the time needed for full exchange of the solutions inside the recording chamber (Fig. 5E).

In conclusion, AGs rapidly enter OHCs in a voltage-dependent manner, indicating permeation through MET channels. Moreover, the kinetics of AG entry into OHCs are consistent with the rapid inhibition of $I_{K,n}$ observed under similar experimental conditions.

AG-Induced Inhibition of $I_{K,n}$ Depolarizes OHCs. Loss of functional KCNQ4, and therefore $I_{K,n}$, results in OHC loss. The mechanisms that couple reduced $I_{K,n}$ to hair cell degeneration are not fully understood, but it seems likely that depolarization and subsequent Ca^{2+} overload play a major role (Oliver et al., 2003; Kharkovets et al., 2006), because $I_{K,n}$ is the principal determinant of membrane potential of OHCs (Marcotti and Kros, 1999; Kharkovets et al., 2006). Therefore, we next monitored membrane potential to investigate the immediate consequences of AG-mediated inhibition of $I_{K,n}$ (Fig. 6).

Under control conditions, membrane potentials of OHCs were constant during whole-cell recordings (V_M change, +0.4 ± 0.2 mV at 10 min after establishing the whole-cell configuration; $n = 8$). In contrast, neomycin (1 mM) depolarized OHCs both when introduced via the patch pipette (by +7.0 ± 2.4 mV; $n = 6$) and when applied from the extracellular side (+5.5 ± 1.0 mV; $n = 14$). Fully blocking $I_{K,n}$ resulted in even stronger depolarization of OHCs by +26.8 ± 3.4 mV ($n = 4$), as assessed by application of the KCNQ-specific antagonist XE991 (10 μM). Kanamycin and G418 had a small, albeit not significant, depolarizing effect when applied through the pipette, and ampicillin was entirely ineffective. Given the presumed relevance of depolarization in OHC degeneration upon dysfunction of KCNQ4, these findings point to $I_{K,n}$ inhibition as a mechanism contributing to AG ototoxicity.

Rescue of $I_{K,n}$ from Inhibition by Chemical KCNQ Channel Openers. If inhibition of $I_{K,n}$ contributes to hair cell loss, the reversal of current block by recently discovered activators of KCNQ channels (Wulff et al., 2009) might provide protection against AG ototoxicity. Therefore, we examined whether KCNQ channel openers could be used to rescue the $I_{K,n}$ conductance inhibited by AGs. We tested the channel openers retigabine (Rundfeldt and Netzer, 2000) and zinc pyrithione (ZnP) (Xiong et al., 2007). Both compounds slightly enhanced $I_{K,n}$ in the presence of intracellular neomycin (500 μM) at concentrations of up to 10 μM (Supplemental Fig. S3). However, combined application of retigabine and ZnP (10 μM each) robustly enhanced $I_{K,n}$ amplitudes (Fig. 7A).

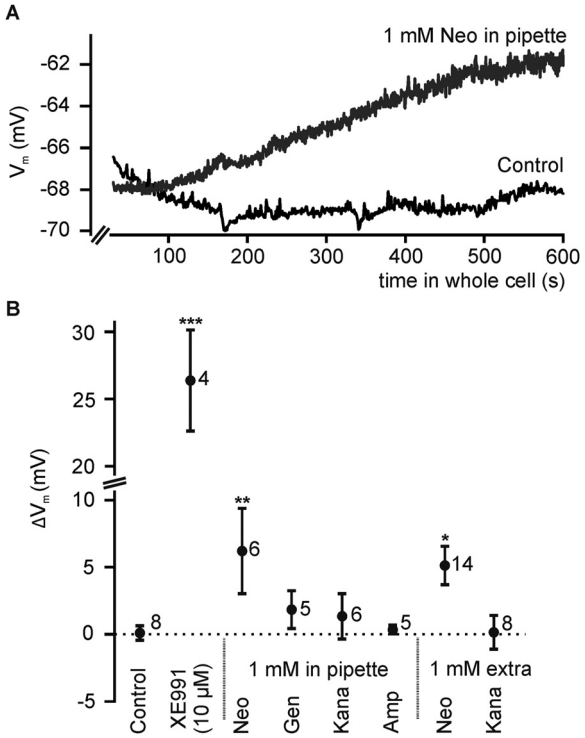

Fig. 6. Neomycin depolarizes OHCs. A, representative recordings of OHC membrane potential in current clamp mode. Patch pipettes contained either standard intracellular solution (control) or additional 1 mM neomycin. The establishment of whole-cell configuration at $t = 0$. B, summary of membrane potential changes, recorded as in A upon application of XE991, aminoglycosides or ampicillin, either via the patch pipette or by application through the extracellular solution as indicated. Note robust depolarization by intracellular and extracellular neomycin. *, $P \leq 0.05$; **; $P \leq 0.01$; ***, $P \leq 0.001$.

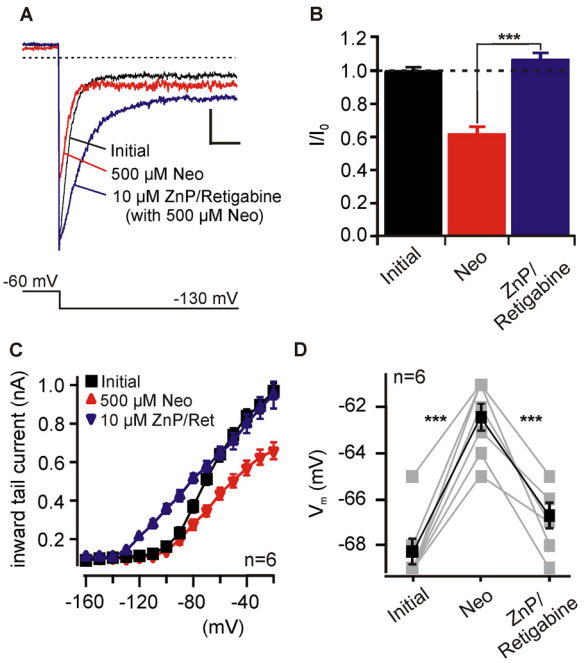

Fig. 7. Rescue of $I_{K,n}$ currents by chemical channel openers. A, representative $I_{K,n}$ tail currents recorded from an OHC immediately after patch rupture (black; control), after dialysis of neomycin from the patch pipette into the cell (red), and during additional extracellular application of zinc pyrithione (ZnP) and retigabine (10 μM each; blue) (scale bars represent 200 pA and 50 ms). B, averaged current amplitudes, obtained as in A at a membrane potential of −70 mV. Note the full reversal of neomycin-induced $I_{K,n}$ inhibition by ZnP plus retigabine. C, mean I-V curves for $I_{K,n}$, obtained from tail currents at −130 mV and plotted as a function of prepulse voltage. Experimental conditions correspond to A and B ($n = 6$). D, OHC membrane potentials measured with a pipette containing 0.5 mM neomycin shortly after establishment of whole-cell conditions, after neomycin diffusion into the cell and during additional extracellular application of ZnP plus retigabine (10 μM each). Gray symbols signify the recordings from individual OHCs and average potentials for each condition are shown in black. Note the reversal of aminoglycoside-induced depolarization by the channel openers. ***, $P \leq 0.001$.

At a physiological membrane potential of −70 mV, the channel activators fully recovered $I_{K,n}$ current to the control amplitude before dialysis of neomycin into the OHCs (Fig. 7, B and C). Accordingly, AG-induced depolarization was largely reversed by the application of the channel openers (Fig. 7D). The effects on current amplitude and membrane potential resulted exclusively from the openers' action on $I_{K,n}$, because increase of OHC currents was fully occluded in the presence of the specific KCNQ channel blocker XE991 (Supplemental Fig. S4). Current enhancement by the channel openers resulted from an increase in saturating $I_{K,n}$ conductance and from a pronounced leftward shift of the activation curve (Fig. 7D and Supplemental Fig. S5). Thus, application of retigabine plus ZnP induced an over-recovery of $I_{K,n}$ at potentials more negative than −70 mV (Fig. 7C). In conclusion, these results show that chemical KCNQ openers can reverse the inhibition of $I_{K,n}$ by AGs and stabilize the OHC membrane potential despite AG entry.

Discussion

Inhibition of KCNQ4-Mediated $I_{K,n}$ via PI(4,5)P_2 Sequestration. Here, we show for the first time that AGs have an immediate inhibiting effect on the major K^+ conductance of OHCs, $I_{K,n}$. Moreover, we demonstrate that the mechanism underlying current deactivation is the decrease of free plasma membrane PI(4,5)P_2 as a result of sequestration by AGs. This conclusion is consistent with a recent report showing that intracellular polycations, including neomycin, can inhibit heteromeric KCNQ2/3 channels by electrostatic interaction with PI(4,5)P_2 (Suh and Hille, 2007). Adding to the previous work, our data strongly support this mechanism of $I_{K,n}$ inhibition by directly demonstrating that AGs efficiently bind to membrane PI(4,5)P_2 using a fluorescent PI(4,5)P_2 sensor, Tubby (Santagata et al., 2001). The potency of different AGs to inhibit KCNQ4 correlates with the strength of PI(4,5)P_2 binding, derived from their efficacy in displacing Tubby. Moreover, the susceptibility to AG-induced block of different KCNQ channel isoforms is in agreement with their distinct PI(4,5)P_2 affinities as determined previously using independent methods (Li et al., 2005; Hernandez et al., 2009). $I_{K,n}$ seemed moderately less sensitive to the depletion of PI(4,5)P_2 induced by intracellularly applied AGs compared with recombinant KCNQ4. Different possible explanations may be considered. First, diffusional access of AGs to the PI(4,5)P_2 pool associated with the channels may be restricted (e.g., by subsurface cisternae, lamellar membrane sheets that are tightly stacked below the lateral plasma membrane). However, the localization of KCNQ4 has only little overlap with the membrane regions associated with cisternae (Kharkovets et al., 2000). Second, OHCs may possess higher basal PI(4,5)P_2 concentrations than mammalian culture cells such as CHO cells. Finally, the PI(4,5)P_2 affinity of native $I_{K,n}$ channels may differ from recombinant KCNQ4. Pronounced differences between $I_{K,n}$ and recombinant channels have been noted previously. In particular, native channels are characterized by a strikingly more negative activation range and faster kinetics (Kubisch et al., 1999; Marcotti and Kros, 1999). The present data extend these differences, suggesting a functional adjustment of KCNQ4 in OHCs (e.g., by post-translational modification or accessory channel subunits).

Mechanism of AG Entry into Hair Cells. Inhibition of $I_{K,n}$ by extracellular neomycin indicated rapid uptake into the OHC cytosol, supporting the existence of a hair cell-specific entry pathway for AGs. Uptake of AGs into hair cells has been determined as the first step leading to the ototoxic action of AGs (Forge and Schacht, 2000), and two different mechanisms for entry of AGs into hair cells have been suggested: endocytotic uptake at the apical surface (de Groot et al., 1990; Hashino and Shero, 1995), or permeation through the MET channels located in the stereocilia (Marcotti et al., 2005).

Our data strongly support entry through MET channels: the rapid inhibition of $I_{K,n}$ and the rapid uptake of fluorescent NTR are difficult to reconcile with endocytosis. Moreover, PI(4,5)P_2 sequestration requires cytosolic localization of free AGs immediately after uptake, whereas endocytosis would deliver AGs into the lumen of organelles. Accordingly, the increase of fluorescence was first detected in the hair bundle, followed by slower accumulation of NTR in the apical pole of the OHC. This indicates that the hair bundle, but not the apical surface, is the site of AG entry. Finally, the observed voltage dependence of entry is consistent with electrically driven permeation.

The mode of AG entry has important implications for the intracellular concentration that can be reached at a given extracellular concentration. We show here that some 100 μM intracellular neomycin is required to substantially inhibit $I_{K,n}$. A comparable degree of inhibition resulted from the application of 1 mM extracellular neomycin. However, systemic administration of AGs yields lower endolymphatic concentrations in the micromolar range (de Groot et al., 1990; Marcotti et al., 2005). Can this result in relevant reduction of $I_{K,n}$?

In vivo, membrane potential and endocochlear potential provide a −150-mV electrical driving force for cation entry into the hair cell, which allows for the generation of huge concentration gradients. Maximum intracellular concentration is reached at electrochemical equilibrium, which is quantitatively described by the Nernst equation. For a tetravalent cation such as neomycin (valence 4.5 at pH 7), the calculated potential intracellular concentration would exceed extracellular concentration by approximately 10^{10} at an electrical driving force of −150 mV. Using the dihydrostreptomycin entry rate estimated by Marcotti et al. (2005) of 0.05 fmol/h at an extracellular concentration of 1 μM, intracellular concentrations of several hundred micromoles may be reached within hours. Thus, even micromolar endolymphatic concentrations can produce intracellular concentrations that result in massive inhibition of $I_{K,n}$. It is noteworthy that, because of the endocochlear potential, the electrical driving force is much larger in vivo than in the patch-clamp and imaging experiments presented here, allowing for higher cytoplasmic accumulation. Yet, cytoplasmic accumulation can be appreciated from NTR uptake, in which intracellular NTR fluorescence rapidly exceeds extracellular fluorescence.

Inhibition of $I_{K,n}$ and AG Ototoxicity. Strikingly, the interaction of AGs with phosphoinositides as a potential mechanism underlying AG-induced hair cell loss was recognized approximately three decades ago (Lodhi et al., 1980). Our data now identify KCNQ4, the channel that mediates $I_{K,n}$, as a molecular target affected by AG-phosphoinositide interaction. Other channels present in OHCs were not af-

fected by aminoglycosides (Supplemental Fig. S1), or their loss does not affect OHC survival (Vetter et al., 1999; Murthy et al., 2009). Because it is well documented that $I_{K,n}$ is essential for the survival of OHCs (Nouvian et al., 2003; Kharkovets et al., 2006), it seems likely that AG-induced inhibition of this current contributes to ototoxicity.

This idea is supported by a conspicuous correlation between the ototoxic potency of AG antibiotics and their efficacy in inhibiting $I_{K,n}$. Thus, neomycin exhibits higher cochleotoxicity than gentamicin and kanamycin in vivo and in vitro (Lodhi et al., 1980). Likewise, vulnerability to AGs of the different hair cell types correlates well with the expression of KCNQ4 and the requirement of KCNQ4 for cell survival. Most obviously, the highest susceptibility to damage by AGs is found in OHCs, in which KCNQ4/$I_{K,n}$ provides essentially all of the resting K^+ conductance (Marcotti and Kros, 1999; Kharkovets et al., 2006). Moreover, the higher vulnerability of basal OHCs that results in the characteristic high-frequency hearing loss upon administration of AGs (Fausti et al., 1984), corresponds to a base-to-apex gradient of KCNQ4 expression (Kharkovets et al., 2000) and $I_{K,n}$ conductance (Mammano and Ashmore, 1996). We have shown previously that IHC express KCNQ4, in which it contributes to setting the membrane potential (Oliver et al., 2003). However, IHC function and survival do not obviously depend on this current (Nouvian et al., 2003; Kharkovets et al., 2006). In agreement with this difference to OHCs, IHCs are little, if at all, affected by AGs (Forge and Schacht, 2000).

A similar correlation is found for vestibular hair cells. Here, KCNQ4 is specifically expressed in type I but not in type II cells (Kharkovets et al., 2000). In analogy to cochlear hair cells, KCNQ4-expressing type I cells are more susceptible to AG-induced hair cell death (Forge and Schacht, 2000). It remains to be shown whether KCNQ-mediated currents in vestibular type I hair cells are inhibited by AGs and whether KCNQ4 is required for their survival.

Despite these considerations, it seems unlikely that inhibition of $I_{K,n}$ is the unique or predominant cause of AG-induced hair cell loss. Detailed analyses have demonstrated that multiple intracellular signaling pathways mediate OHC death by necrotic and/or apoptotic mechanisms (Jiang et al., 2006a). Considerable evidence, both from in vitro and in vivo experiments, points to the generation of reactive oxygen species as a major mechanism leading to AG-induced hair cell loss (Forge and Schacht, 2000). Additional mechanisms such as phospholipid scrambling triggered by interaction of AGs with phosphoinositides (Goodyear et al., 2008) may contribute as well. At present, it is not known how impairment of KCNQ4-mediated currents leads to OHC loss. However, cellular depolarization may be critical, possibly by initiating voltage-dependent Ca^{2+} influx (Oliver et al., 2003; Kharkovets et al., 2006). Excessive intracellular Ca^{2+} is involved in triggering several signals that promote cell death (Stefanis, 2005). It is noteworthy that such Ca^{2+}-sensitive signals have been implicated in AG-induced hair cell death, including the activation of calpain and subsequent release of cathepsins (Jiang et al., 2006a). Moreover, increased intracellular Ca^{2+} can contribute to mitochondrial dysfunction, which is implicated in hair cell degeneration (Dehne et al., 2002).

In conclusion, AG-induced depolarization may add to and act cooperatively with previously identified mechanisms of hair cell death. We propose that the dependence of outer hair cells on KCNQ-mediated conductances may be an important determinant of their vulnerability to AGs.

Rescue of $I_{K,n}$ by KCNQ Channel Openers. Given that insufficient KCNQ4 activity leads to the degeneration of OHCs (Nouvian et al., 2003; Kharkovets et al., 2006), strategies for the prevention of current inhibition might have important therapeutic potential. Here, we demonstrate that the chemical KCNQ openers retigabine and zinc pyrithione enhance $I_{K,n}$ in OHCs and fully reverse inhibition by AGs.

Retigabine is being evaluated for use as an anticonvulsant drug in clinical trials (Wulff et al., 2009). In addition, potential clinical applications of retigabine and other recently identified KCNQ channel activators include treatment of pain and neuropsychiatric conditions (Wulff et al., 2009). Our data suggest that KCNQ activators may be evaluated for antagonism of AG ototoxicity. Despite the requirement of relatively high concentrations of channel activators (10 μM) for $I_{K,n}$ rescue, the recent discovery and ongoing development of further KCNQ openers (Wulff et al., 2009) seems promising with respect to compounds with improved potency for $I_{K,n}$ enhancement. Moreover, the combinatorial action of different channel openers may increase their therapeutic potential in inner ear disease. Additive current enhancement by retigabine and zinc pyrithione was described previously for recombinant neuronal KCNQ2 channels (Xiong et al., 2008). The combinatorial effect seems to result from simultaneous binding to distinct binding sites, and distinct molecular determinants for the action of each channel opener have been identified (Xiong et al., 2008). Because the determinant amino acid residues are fully conserved between KCNQ2 and KCNQ4, we presume that binding sites and mechanism of action on $I_{K,n}$ are the same as identified previously for KCNQ2 channels.

We note that KCNQ4 openers might be useful in further conditions leading to hearing loss as a result of OHC degeneration. It will be interesting to see whether the openers can rescue the phenotype of human KCNQ4 mutations underlying DFNA2, similar to the rescue of epileptogenic mutations of KCNQ2 (Xiong et al., 2007). Moreover, correlations between KCNQ4 gene polymorphisms and both age-related and noise-induced hearing loss have been found (Van Eyken et al., 2006), suggesting that rather subtle changes in KCNQ4 expression or function may contribute to deafness. Thus, these frequent conditions might benefit from drugs modulating KCNQ4-mediated currents. In summary, the present data suggest that the spectrum of potential therapeutic use of KCNQ channel activators may include hearing loss.

Acknowledgments

cDNA constructs were kindly provided by Drs. Thomas Jentsch (Leibniz Institut für Molekulare Pharmakologie FMP and Max Delbrück Centrum für Molekulare Medizin MDC, Berlin, Germany; KCNQ4 and KCNQ3) and Lawrence Shapiro (Department of Biochemistry and Molecular Biophysics, Columbia University, New York, NY; tubby-Cterm). We gratefully acknowledge excellent technical assistance by O. Ebers and S. Petzold.

Authorship Contributions

Participated in research design: Leitner, Halaszovich, and Oliver.
Conducted experiments: Leitner.
Contributed new reagents or analytic tools: Halaszovich.
Performed data analysis: Leitner and Oliver.
Other: Oliver acquired funding for the research.

References

Dai CF, Mangiardi D, Cotanche DA, and Steyger PS (2006) Uptake of fluorescent gentamicin by vertebrate sensory cells in vivo. *Hear Res* **213:**64–78.

de Groot JC, Meeuwsen F, Ruizendaal WE, and Veldman JE (1990) Ultrastructural localization of gentamicin in the cochlea. *Hear Res* **50:**35–42.

Dehne N, Rauen U, de Groot H, and Lautermann J (2002) Involvement of the mitochondrial permeability transition in gentamicin ototoxicity. *Hear Res* **169:** 47–55.

Fausti SA, Rappaport BZ, Schechter MA, Frey RH, Ward TT, and Brummett RE (1984) Detection of aminoglycoside ototoxicity by high-frequency auditory evaluation: selected case studies. *Am J Otolaryngol* **5:**177–182.

Forge A and Schacht J (2000) Aminoglycoside antibiotics. *Audiol Neurootol* **5:**3–22.

Gabev E, Kasianowicz J, Abbott T, and McLaughlin S (1989) Binding of neomycin to phosphatidylinositol 4,5-bisphosphate (PIP2). *Biochim Biophys Acta* **979:**105–112.

Goodyear RJ, Gale JE, Ranatunga KM, Kros CJ, and Richardson GP (2008) Aminoglycoside-induced phosphatidylserine externalization in sensory hair cells is regionally restricted, rapid, and reversible. *J Neurosci* **28:**9939–9952.

Halaszovich CR, Schreiber DN, and Oliver D (2009) Ci-VSP is a depolarization-activated phosphatidylinositol-4,5-bisphosphate and phosphatidylinositol-3,4,5-trisphosphate 5′-phosphatase. *J Biol Chem* **284:**2106–2113.

Hashino E and Shero M (1995) Endocytosis of aminoglycoside antibiotics in sensory hair cells. *Brain Res* **704:**135–140.

Hernandez CC, Falkenburger B, and Shapiro MS (2009) Affinity for phosphatidylinositol 4,5-bisphosphate determines muscarinic agonist sensitivity of Kv7 K^+ channels. *J Gen Physiol* **134:**437–448.

Hiel H, Erre JP, Aurousseau C, Bouali R, Dulon D, and Aran JM (1993) Gentamicin uptake by cochlear hair cells precedes hearing impairment during chronic treatment. *Audiology* **32:**78–87.

Jiang H, Sha SH, Forge A, and Schacht J (2006a) Caspase-independent pathways of hair cell death induced by kanamycin in vivo. *Cell Death Differ* **13:**20–30.

Jiang H, Sha SH, and Schacht J (2006b) Kanamycin alters cytoplasmic and nuclear phosphoinositide signaling in the organ of Corti in vivo. *J Neurochem* **99:**269–276.

Kharkovets T, Dedek K, Maier H, Schweizer M, Khimich D, Nouvian R, Vardanyan V, Leuwer R, Moser T, and Jentsch TJ (2006) Mice with altered KCNQ4 K^+ channels implicate sensory outer hair cells in human progressive deafness. *EMBO J* **25:**642–652.

Kharkovets T, Hardelin JP, Safieddine S, Schweizer M, El-Amraoui A, Petit C, and Jentsch TJ (2000) KCNQ4, a K^+ channel mutated in a form of dominant deafness, is expressed in the inner ear and the central auditory pathway. *Proc Natl Acad Sci USA* **97:**4333–4338.

Kubisch C, Schroeder BC, Friedrich T, Lütjohann B, El-Amraoui A, Marlin S, Petit C, and Jentsch TJ (1999) KCNQ4, a novel potassium channel expressed in sensory outer hair cells, is mutated in dominant deafness. *Cell* **96:**437–446.

Li Y, Gamper N, Hilgemann DW, and Shapiro MS (2005) Regulation of Kv7 (KCNQ) K^+ channel open probability by phosphatidylinositol 4,5-bisphosphate. *J Neurosci* **25:**9825–9835.

Lodhi S, Weiner ND, Mechigian I, and Schacht J (1980) Ototoxicity of aminoglycosides correlated with their action on monomolecular films of polyphosphoinositides. *Biochem Pharmacol* **29:**597–601.

Mammano F and Ashmore JF (1996) Differential expression of outer hair cell potassium currents in the isolated cochlea of the guinea-pig. *J Physiol* **496:**639–646.

Marcotti W and Kros CJ (1999) Developmental expression of the potassium current IK,n contributes to maturation of mouse outer hair cells. *J Physiol* **520:**653–660.

Marcotti W, van Netten SM, and Kros CJ (2005) The aminoglycoside antibiotic dihydrostreptomycin rapidly enters mouse outer hair cells through the mechano-electrical transducer channels. *J Physiol* **567:**505–521.

Murthy V, Maison SF, Taranda J, Haque N, Bond CT, Elgoyhen AB, Adelman JP, Liberman MC, and Vetter DE (2009) SK2 channels are required for function and long-term survival of efferent synapses on mammalian outer hair cells. *Mol Cell Neurosci* **40:**39–49.

Nouvian R, Ruel J, Wang J, Guitton MJ, Pujol R, and Puel JL (2003) Degeneration of sensory outer hair cells following pharmacological blockade of cochlear KCNQ channels in the adult guinea pig. *Eur J Neurosci* **17:**2553–2562.

Oliver D, Klöcker N, Schuck J, Baukrowitz T, Ruppersberg JP, and Fakler B (2000) Gating of Ca^{2+}-activated K^+ channels controls fast inhibitory synaptic transmission at auditory outer hair cells. *Neuron* **26:**595–601.

Oliver D, Knipper M, Derst C, and Fakler B (2003) Resting potential and submembrane calcium concentration of inner hair cells in the isolated mouse cochlea are set by KCNQ-type potassium channels. *J Neurosci* **23:**2141–2149.

Oliver D, Lien CC, Soom M, Baukrowitz T, Jonas P, and Fakler B (2004) Functional conversion between A-type and delayed rectifier K^+ channels by membrane lipids. *Science* **304:**265–270.

Rundfeldt C and Netzer R (2000) The novel anticonvulsant retigabine activates M-currents in Chinese hamster ovary-cells transfected with human KCNQ2/3 subunits. *Neurosci Lett* **282:**73–76.

Rybak LP and Ramkumar V (2007) Ototoxicity. *Kidney Int* **72:**931–935.

Sandoval R, Leiser J, and Molitoris BA (1998) Aminoglycoside antibiotics traffic to the Golgi complex in LLC-PK1 cells. *J Am Soc Nephrol* **9:**167–174.

Santagata S, Boggon TJ, Baird CL, Gomez CA, Zhao J, Shan WS, Myszka DG, and Shapiro L (2001) G-protein signaling through tubby proteins. *Science* **292:**2041–2050.

Stefanis L (2005) Caspase-dependent and -independent neuronal death: two distinct pathways to neuronal injury. *Neuroscientist* **11:**50–62.

Suh BC and Hille B (2007) Electrostatic interaction of internal Mg^{2+} with membrane PIP2 seen with KCNQ K^+ channels. *J Gen Physiol* **130:**241–256.

Suh BC, Inoue T, Meyer T, and Hille B (2006) Rapid chemically induced changes of PtdIns(4,5)P2 gate KCNQ ion channels. *Science* **314:**1454–1457.

Tiede L, Steyger PS, Nichols MG, and Hallworth R (2009) Metabolic imaging of the organ of Corti–a window on cochlea bioenergetics. *Brain Res* **1277:**37–41.

Van Eyken E, Van Laer L, Fransen E, Topsakal V, Lemkens N, Laureys W, Nelissen N, Vandevelde A, Wienker T, Van De Heyning P, et al. (2006) KCNQ4: a gene for age-related hearing impairment? *Hum Mutat* **27:**1007–1016.

Vetter DE, Liberman MC, Mann J, Barhanin J, Boulter J, Brown MC, Saffiote-Kolman J, Heinemann SF, and Elgoyhen AB (1999) Role of alpha9 nicotinic ACh receptor subunits in the development and function of cochlear efferent innervation. *Neuron* **23:**93–103.

Wang Q and Steyger PS (2009) Trafficking of systemic fluorescent gentamicin into the cochlea and hair cells. *J Assoc Res Otolaryngol* **10:**205–219.

Wulff H, Castle NA, and Pardo LA (2009) Voltage-gated potassium channels as therapeutic targets. *Nat Rev Drug Discov* **8:**982–1001.

Xiong Q, Sun H, and Li M (2007) Zinc pyrithione-mediated activation of voltage-gated KCNQ potassium channels rescues epileptogenic mutants. *Nat Chem Biol* **3:**287–296.

Xiong Q, Sun H, Zhang Y, Nan F, and Li M (2008) Combinatorial augmentation of voltage-gated KCNQ potassium channels by chemical openers. *Proc Natl Acad Sci USA* **105:**3128–3133.

Address correspondence to: Dr. Dominik Oliver, Department of Neurophysiology, Institute for Physiology and Pathophysiology, Philipps-Universität Marburg, Deutschhausstr. 2, 35037 Marburg, Germany, E-mail: oliverd@staff.uni-marburg.de